Open access • Journal Article • DOI:10.1179/174328408X385773

Plasticity induced transformation in a metastable β Ti-1023 alloy by controlled heat treatments — Source link

Suresh Neelakantan, D. San Martín, Pedro E.J. Rivera-Díaz-del-Castillo, S. van der Zwaag

Institutions: Delft University of Technology

Published on: 01 Nov 2009 - Materials Science and Technology (Maney Publishing)

Plasticity Induced Transformation in a metastable β Ti-1023 alloy by controlled heat treatments

Suresh Neelakantan[1,2,*], David San Martin[1,2], Pedro E.J. Rivera-Díaz-del-Castillo[2] and Sybrand van der Zwaag[2]

[1]*Netherlands Institute for Metals Research, Mekelweg 2, 2600 GA, Delft, The Netherlands*

[2]*Faculty of Aerospace Engineering, Delft University of Technology, Kluyverweg 1, 2629 HS, Delft, The Netherlands*

Abstract:

Investigations into the possibility of improving the strength-ductility relation in a metastable β-titanium alloy (Ti-10V-2Fe-3Al) through plasticity induced transformation (PiTTi) have been carried out. Various heat treatments in the β and/or $\alpha+\beta$ condition were performed to study their influence on both the microstructure and solute partitioning, which eventually control the PiTTi effect. Stress-induced martensite formation promoting such effect has been observed upon compression testing for β and $\beta+(\alpha+\beta)$ microstructures. The stress-strain curves exhibiting stress-induced martensite show ~20% increase in strength, while still retaining a reasonable ductility level. Microstructural parameters such as grain size and solute concentration (especially V) in β have been related to the alloy's ability to exhibit PiTTi.

Keywords: Titanium; Heat treatment; Microstructure; Martensitic transformation; Mechanical properties;

[*] Author for correspondence. Phone: +31-15-2785218; Fax: +31-15-2784472.
e-mail: s.neelakantan@tudelft.nl

1. Introduction

β-metastable titanium alloys possess a high strength-to-density ratio, relatively low thermomechanical processing costs, good hardenability, forgeability and high temperature resistance. However, their success in commercial applications is restricted due to the limited cold formability; for example, β titanium alloys displaying fine α and ω particles in the microstructure show limited elongation upon deformation.[1,2] This limitation can be addressed via promoting the formation of stress-induced martensite. In ferrous alloys, the stress- or strain-induced martensite of metastable austenite has provided an improved balance of strength and ductility.[3-5] The effect of mechanically activated martensitic transformation of metastable austenite in steels is commonly referred to as transformation induced plasticity (TRIP).[4] Recent studies in β titanium alloys like β-Cez,[7] Ti-V-Fe-Al,[8] Ti-V[9] and Ti-Ta[10] have shown evidence of similar mechanism, which is termed here Plasticity induced Transformation in Titanium (PiTTi).

It is generally accepted that β titanium alloys may undergo deformation via the formation of stress-induced martensite (SIM).[2,11-14] This mechanism, along with slip and twinning, could provide improved strength-ductility relationships. The formation of martensite due to the application of load depends on the microstructural state of the alloy and in particular the β phase stability.[8,11] In analogy to ferrous alloys (multiphase steels), the ability of the high temperature phase (β) to deform martensitically at room temperature can be controlled by tailoring the local concentrations via well designed heat treatments.[2,7,15] Of prime importance is understanding the effects of the local concentration variation of the

alloying elements and the deformation state, which results from the various thermomechanical schedules.[16,17] These factors determine the ability to undergo SIM deformation at room temperature, which is the deformation mechanism behind the PiTTi effect.

The metastable β alloys show a good response to heat treatment and their microstructures can be easily modified. This should permit the tuning of microstructural parameters to achieve an optimized PiTTi effect, improving mechanical properties.[7,18] There has been, however, no general survey on the control of the conditions leading to an optimization of strength-ductility relationships in Ti alloys undergoing the plasticity induced transformation to martensite. By considering various heat treatment scenarios to control the microstructure, the present work aims at exploring the possibilities of improving the strength and ductility relationships.

2. Experimental methods

The β-metastable titanium alloy, Ti-10V-2Fe-3Al (wt.%) (Ti-1023), was obtained from TIMET, Germany. The compositional analysis conducted by the supplier is shown in Table 1. The β-transus temperature of this alloy is 795±5 °C.[8,18] The alloy displayed a bimodal $\alpha+\beta$ microstructure in its as-received condition (Fig. 1c). The as-received pancake was produced by i) forging the ingot at β-transus temperature + 30 °C, and then at 750 °C, where the bi-modal distribution was formed; this was followed with ii) a heat treatment at 760 °C for 1h, water quenched and then aged at 525 °C for 8h, air cooled. The as-received pancake was

further shaped using electrical discharge machining (EDM) into cylindrical samples of 4 mm diameter and 7 mm length. The samples were heat treated at several temperatures and times in the β and/or $\alpha+\beta$ domains using a Bähr 805 horizontal dilatometer at a vacuum level of 10^{-5} mbar, and quenched to room temperature by Helium gas. The heating and cooling rate were 10 °C/s. The martensite transformation temperatures after each heat treatment were measured with the dilatometer. The high quenching rate (~400 °C/s) achieved by the injection of high pressure Helium, however, distorts the dilation signal making it difficult for the precise identification of the M_s. Moreover, a large scattering has been observed in the transition temperatures in titanium alloys due to segregation.[19] The heat treated samples were microstructurally characterized using optical and scanning electron microscopy. Prior to that, the samples were i) electropolished in a solution of perchloric acid, methanol, ethylene glycol and water, and ii) etched with Kroll's reagent ($HF+HNO_3$+water).

The identification of the phases present in the heat treated and compressed microstructures has been carried out using X-ray diffraction (XRD) with Co K_α radiation at room temperature. XRD data were taken from the longitudinal cross section of the samples. Electron probe micro analysis (EPMA) was performed in a JEOL JXA 8900R microscope to track the local concentration variations in the microstructures. The concentration data were obtained using a 15 kV, 50 nA beam. The local concentrations of the major constitutive elements (V, Al, Fe and Ti) have been measured. To study the stress-induced martensite (SIM) formation ability, compression testing of the samples was carried out using the Gleeble®1500

machine. The samples were deformed at room temperature to different strain levels varying from 5 to 40 % at a strain rate of 10^{-3} s^{-1}.

3. Results

3.1) Heat treatment effects

A comprehensive study has been carried out to determine the influence of heat treatments on the microstructure kinetics and on its resulting solute partitioning effects. Table 2 summarizes the heat treatment schedules applied to the Ti-1023 samples. The heat treatment temperatures were chosen in the β, $\alpha+\beta$ and $\beta+(\alpha+\beta)$ phase fields.

3.1.1) β phase field

The above β-transus experiments were conducted at various temperatures from 800 to 1100 °C (Table 2). Almost all above β heat treatments did not yield 100% metastable β at room temperature, as the quenched microstructures showed athermal martensite formation (Fig. 1a). Similar results were reported by Duerig *et al.*[18] Temperature variations within the β region led to microstructures differing in grain size and the volume fraction of the martensite. In general, higher temperatures or longer times resulted in larger β grain sizes with a lower volume fraction of athermal martensite. Their presence was restricted to the neighbourhood of grain boundaries.

3.1.2) $\alpha+\beta$ phase field

The below β-transus treatment was performed at 700 °C for 15 min. It resulted in a bi-modal microstructure with a mixture of α and β phases. The α appears in a globular form and as laths embedded in a β matrix. The microstructure of the alloy is shown in Figure 1b. Further, with increasing temperature or time within the α+β domain, the α laths dissolve, leaving only globular α with a lower volume fraction and more retained β domains.[2] The microstructure of Figure 1b is thus a transition between the as-received condition (Fig. 1c) and predominantly globular α with retained β domains.

3.1.3) β+(α+β) phase field

In this particular treatment, the samples were solutionised in the β regime and cooled to the α+β region, soaked and subsequently quenched. Table 2 lists the heat treatment temperatures and times explored. The aim of these experiments was to study the influence of the α phase on the β stability. The quenched samples show predominantly α grains possessing different morphologies: laths inside the grains and Widmanstätten near prior β grain boundaries.[20] An increase in temperature and time within the β field resulted in large prior β grains. Within the β grains, depending on the temperature and time in the α+β regime, α of both morphologies encompassed the grains. The upper α+β temperatures (just below β transus temperature) resulted in more untransformed metastable β domains (Fig. 1d) upon quenching as compared to the lower α+β temperatures (far below β transus), Fig. 1e.

3.2) Microstructural analysis

Based on their microstructural features, the detailed characterization of three selected heat treatments was performed: A) 900 °C-60min *(β)*, B) 700 °C-15min *(α+β)*, C) 900 °C-15min/700 °C-15min *(β+(α+β))* and D) 900 °C-15min/650 °C-15min *(β+(α+β))*; referred hereafter as samples A, B, C and D respectively.

3.2.1 X-ray investigation

A detailed analysis has been carried out using XRD to identify and confirm the phases present in the microstructures of the samples A, B and C. Figure 2 shows the corresponding diffractograms. The peaks indicate that the phases present in these samples are α, α', α'' and β, and their respective lattice parameters are given in Table 3. The corresponding microstructures of the XRD investigated samples are given in Figures 1a, 1b and 1e. α'' peaks were observed only for the treatments involving above β temperatures. Similar observations were made by Duerig *et al.*[18] for above β heat treatments. Additionally they reported the presence of ω phase, which was not observed in our studies, at least not from the optical microscopy and XRD results.

3.2.2 EPMA analysis

In order to determine the microstructural and solute partitioning conditions favouring martensite formation, local concentration changes have been measured using EPMA. Such studies were performed on samples A, B and D. Figures 3a to 3c respectively show the traces along which the probe measurements were carried

out; Figures 3d to 3f show the variation in concentration of the major elements, respectively. In Figure 3b the probe measurements were carried out as series of vertical parallel lines labelled as line *1, 2* till line *n*, and their respective concentration variations is given in Fig. 3e, where the region corresponding to line *1* and line *2* is highlighted. This kind of measurement profile was chosen to consider the morphology effect on concentration variation. The results show evidence of partitioning or segregation of the elements within the microstructures for the *(α+β)* and *β+(α+β)* treatments, Figs. 3b, 3e, 3c and 3f. There is no evidence of solute redistribution for the above *β* treated samples (Figs. 3a and 3d), where predominantly metastable *β* and athermal martensite near grain boundaries is present.

3.3) Mechanical property evaluation

The heat treated microstructures were compression tested to evaluate their stress-induced martensite (SIM) formation ability. The samples A) 900 °C-60min *(β)*, B) 700 °C-15min *(α+β)* and C) 900 °C-15min/700 °C-15min *(β+(α+β))* were chosen for the compression testing. It is to be noted that sample C *(β+(α+β))* was chosen other than sample D as optical studies indicated more metastable *β* domains (Fig. 1d) present in sample C. Each heat treated sample was compressed to various strain levels ranging from ~5% to ~40%. Figure 4 shows selected stress-strain curves for the as-received condition and samples A, B and C. Sample A was stopped before failure at ~35% strain and samples B and C failed by macroscopic shearing. Samples A and C show a double yield point-like behaviour, which is

absent in sample B. Such a double yield phenomenon is ascribed to the SIM formation producing the PiTTi effect.[2,8] As the strain is increased, the only observed microstructural change is the further transformation into martensite (Figs. 5a and 5b); Further, the quantitative analysis on the fraction of martensite formed in samples A and C show an increasing trend with strain levels ranging from 5 to 20%. Moreover, X-ray diffraction analysis on the compressed samples shows clear formation of SIM (α''- orthorhombic and α'-hexagonal), Fig. 6; Table 3 shows the respective lattice parameters of the phases after compression. Further, samples A and C show an increase in strength by a noticeable amount (~20%), while still retaining a reasonable compressive failure strain. Contrary to samples A and C, the multiphase microstructures of the as-received and sample B (not displaying martensite formation after compression, both confirmed by the optical microscope, Fig. 5c and X-ray diffraction, Fig. 6), did not show the double yield behaviour,[8] ruling out the work hardening change due to multiphase effects. However, this particular treatment has shown large failure strain, although lower strength, than the PiTTi exhibiting heat treatments.

4. Discussion

Three families of heat treatments have been considered in this work: above β transus, $\alpha+\beta$ and $\beta+(\alpha+\beta)$. They show strong differences in their kinetic behaviour resulting in significant microstructural inhomogeneties as summarized in Table 2. The relationship between microstructure and the formation of martensite is related to the stability of β phase, its grain size and the M_s

temperature. There are two factors contributing to the β stabilisation: the concentration of β stabilisers (V and Fe) within that phase and the prior β grain size.[7,8] While V and Fe take a prominent role for bulky grains, grain size[7,8] seems to take over for smaller grains.

The above β transus treatments were expected to result in stable retained β grains. However, a partially transformed microstructure with β and athermal martensite at its grain boundaries (Fig. 1a) was observed.[18] Hence the β was not stable enough to be retained completely at room temperature. EPMA results show concentration fluctuations lower than 0.2 wt.% for Ti, V, Fe and Al (Fig. 3d). Given that the sensitivity of the instrument is lower than ± 0.2 wt.%, it may be concluded that the sample was locally homogenised. The athermal martensite and β regions do not show evidence of solute partitioning, as expected from the diffusionless nature of martensite. The authors have developed a model for predicting the M_s temperature in multi-component Ti alloys, which is based on the composition dependencies of M_s for Ti-V, Ti-Fe and Ti-Al binary systems (Fig. 7),[23-25] and simply averaging between them excluding the ternary and quaternary interactions. This is a modified version of Ghosh and Olson model for martensite formation in ferrous alloys[21] and is reported in detail elsewhere.[22] The observation of athermal α'' martensite for sample A is in accordance with our model calculation. Given the very large β grain size (~300 μm), the micrographs suggest that strong distortions in the crystal structure (grain boundaries) are required for martensite nucleation. Hence decreasing the grain size would increase the volume density of martensite nucleation sites.

The $\alpha+\beta$ microstructure (Fig. 1b) shows a similar bi-modal distribution as the as-received alloy (Fig. 1c), except for a higher volume fraction of β domains. The concentration profiles shown in Figure 3e indicate strong composition fluctuations related to the two phase microstructure. Solute partitioning indicates that β is rich in V and Fe while it is poor in Al. The M_s temperature would locally vary due to the partitioning of the elements. However, no athermal martensite was observed (Fig. 1b) after this treatment. This suggests that (small) β grain size plays a dominant role on the β stability, as has been previously pointed out by other workers.[7,8,26,27] The presence of a large volume fraction of equilibrium α reduces the size of the metastable β grains and stabilizes them; conversely, the large amount of equilibrium α provides a larger amount of interfacial area per unit volume, increasing the volume density of martensite nucleation sites. However, Fig. 1b indicates that the dominant effect is the beta stabilisation due to the small β grain size.

Interesting trends are shown when considering the $\beta+(\alpha+\beta)$ heat treatments. After short homogenisation in the β field (900 °C for 15min) and on further holding in the $\alpha+\beta$ field, two regimes have been distinguished: at 700 °C (Fig. 1d), a small volume fraction of Widmanstätten α is observed next to the grain boundaries, additionally, α flakes are observed along with martensite inside the β grains (sample C); at 650 °C (Fig. 1e), larger amounts of Widmanstätten α encompass the β grains while the grain interior seems to have replaced the martensite by α flakes present at a larger volume fraction (sample D). When

comparing such microstructures to the concentration profile shown in Figure 3f, it may be concluded that at temperatures below β transus (650-700 °C), α diffusionally forms, rejecting V and Fe while absorbing Al. Given that a larger volume fraction of α forms at the lower temperature (650 °C), the remaining small β domains are supersaturated with β stabilizing-isomorphous (V) and eutectoid (Fe) elements; thereby increasing their stability without transformation upon quenching, suggesting the dominant role of the small β grain size on their stability.[7,8,26,27] Whereas, the samples annealed at 700 °C (sample C) show athermal martensite throughout the β grain. The presence of α flakes scattered in the interior of the 700 °C aged $\beta+(\alpha+\beta)$ samples suggests that the β/α-flake interfaces multiply the nucleation sites for martensite, hence the presence of martensite in the interior of such grains.

The alloy microstructure response to the different heat treatment schemes is an aid to understand its plastic deformation ability. The formation of SIM seems to be intrinsically related to the metastability of the β grains.[2,7,8] The present work shows that the PiTTi effect stems from a number of microstructural factors derived from prior heat treatments. Referring to Figure 5a, β undergoes SIM formation as confirmed by the double yield point, which is accompanied by an increase in alloy strength of approximately 20% (Fig. 4). The nature of the SIM formed is α'' orthorhombic[8,18] (Fig. 6). The strength increase may be due to the work hardening of the SIM, which displays a change in the strain hardening exponent. Figure 5b demonstrates that SIM is also formed (Fig. 6) in a $\beta+(\alpha+\beta)$ microstructure (sample C), displaying similar double yield behaviour and peak strength. The solute

concentration in the β phase seems to be consistent with that required to form SIM, this is very similar to that of pure β as indicated in Figure 3d. β+(α+β) microstructures display a larger degree of complexity as shown in Table 2. Higher (α+β) temperatures (700 °C) combine β, martensite, Widmanstätten α and α flakes; the volume fraction of α increases by reducing the (α+β) temperature, increasing the concentration of β stabilisers, and reducing the likelihood of SIM formation. Moreover, the presence of α flakes in the samples aged at 700 °C may be an aid for SIM formation by increasing the volume fraction of its nucleation sites. The absence of SIM in Figure 5c is consistent with the single yield point in Figure 4 for such α+β microstructure, which is very similar to that of the as-received condition. Moreover, the XRD patterns approve the absence of SIM in such microstructure (Fig. 6). The large volume fraction of α stabilise the β grains, precluding the formation of SIM (Fig. 5c).

By comparing Figs. 1a and 5a,b it becomes interesting to note that the obtained SIM displays a very different appearance than the athermal martensite; this nucleates at the grain interfaces and an autocatalytic effect does not seem to appear. In the samples that underwent compression, the grains appear to be fully covered by martensite, suggesting that deformation provides the additional energy fostering the autocatalytic effect. Moreover, the structure of the martensite obtained by deformation is predominantly α'' orthorhombic other than athermally obtained hexagonal martensite.

The work presented here stems from exploring the possibility of reproducing TRIP-like behaviour in steels into titanium alloys. Our observations

show a considerable increase in strength due to PiTTi while retaining a reasonable level of ductility. A key factor for achieving this is by controlling the stability of β. Nevertheless, many additional aspects ought to be considered for improving the mechanical behaviour associated to PiTTi. TRIP steels derive their properties from a soft low temperature phase (ferrite) which is present at a high volume fraction, and supplies ductility. The retained high temperature phase (austenite) is characterised by a larger strength; under deformation, it is transformed into martensite which is even stronger.[28] Conversely, in titanium alloys the low temperature (α) phase usually exhibits a larger strength than its high temperature counterpart (β) and the martensite (α'').[12] An additional increase in ductility in the PiTTi alloys may require an additional phase, e.g. a fraction of beta grains remaining untransformed under deformation due to their change in solute concentration. This may be achieved by imposing an additional step to the thermal processing. The double yield behaviour and the reduced ductility of the PiTTi effect presented here may derive from this. Hence, meticulous tuning of microstructural features is required to achieve the proper balance between β composition and grain size. The addition of interstitial elements may also be explored as a means to strengthen β and martensite. It may result into improved strength-ductility relationships.

5. Conclusions

Detailed studies indicate that plasticity induced martensitic transformation in Ti-1023 alloy can be successfully controlled to achieve improved mechanical

properties. The formation of stress-induced martensite (SIM) is accompanied with double yield point under compression testing, and an increase of ~20% in alloy strength. This was observed in the β and $\beta+(\alpha+\beta)$ alloy microstructures. The ability to undergo such hardening via inducing the formation of SIM seems to be related to the control of the heat treatment temperature and time, and the β concentration, especially that of Vanadium.

Acknowledgements

The financial support from NIMR for this project (MC5.05206) is highly acknowledged. The authors thank Kees Kwakernaak, Nico Geerlofs, Erik Peekstok and Pascal Visser for their help in experimental measurements at various stages during this study.

References

[1] J.C. Williams, B.S. Hickman and H.L. Marcus: *Metall. Trans. A,* 1971, **2A,** 1913-1920.
[2] T.W. Duerig, G.T. Terlinde and J.C. Williams: *Metall. Trans. A,* 1980, **11A,** 1987-1998.
[3] O. Matsumura, Y. Sakura and H. Takechi: *Scripta Metall.,* 1987, **21**, 1301-1306.
[4] K. Sugimoto, N. Usui, M. Kobayashi and S. Hashimoto: *ISIJ intl.,* 1992, **32**, 1311-1318.
[5] P. Jacques, F. Delannay, X. Cornet, P. Harlet and J. Ladriere: *Metall. Mater. Trans. A,* 1998, **29A**, 2383-2393.
[6] P. Jacques, Q. Furnemont, A. Mertens and F. Delannay: *Phil. Mag. A,* 2001, **81**, 1789-1812.
[7] T. Grosdidier, Y. Combres, E. Gautier and M.J. Philippe: *Metall. Mater. Trans. A*, 2000, **31A**, 1095-1106.
[8] A. Bhattacharjee, S. Bhargava, V.K. Varma, S.V. Kamat and A.K. Gogia: *Scripta Mater.*, 2005, **53**, 195-200.
[9] E. Sarath Kumar Menon and R. Krishnan: *J. Mater. Sci.*, 1983, **18,** 365-374.
[10] J.D. Cotton, J.F. Bingert, P.S. Dunn and R.A. Patterson: *Metall. Mater. Trans. A*, 1994, **31A**, 461-472.
[11] T. Grosdidier, C. Roubaud, M.J. Philippe, S. Zaefferer, M. Zandona, E. Gautier and Y. Combres: *J. de Phys. IV*, 1996, **6**, 435-444.
[12] Q.Y. Sun, S.J. Song, R.H. Zhu and H.C. Gu: *J. Mater. Sci.,* 2002, **37**, 2543-2547.
[13] S. Ishiyama, S. Hanada and O. Izumi: *ISIJ intl.,* 1991, **31**, 807-813.
[14] H.M. Flower: Proc. of the 5th Intl. Conf. on Titanium, 1984, 1651.
[15] Alain Vassel: 'Beta Titanium alloys in 1990's', The Minerals, Metals & Materials Society, 1993, (ed. by D.Eylon, R.R.Boyer and D.A. Koss), 173
[16] V.V. Balasubrahmanyam and Y.V.R.K. Prasad: *Mater. Sci. Technol.,* 2001, **17**, 1222-1228.
[17] M.Jackson, R.J. Dashwood, L. Christodoulou and H.M. Flower: *Mater. Sci. Technol.,* 2000, **16**, 1437-1444.
[18] T.W. Duerig, J. Albrecht, D. Richter and P. Fischer: *Acta Metall.*, 1982, **30**, 2161-2172.

[19] S.M.C. van Bohemen, J. Sietsma and S. van der Zwaag: *Phys. Rev. B,* 2006, **74**, 134114.
[20] D. Grandemange, Y. Combres and D. Eylon: 'Beta Titanium alloys in 1990's', The Minerals, Metals & Materials Society, 1993, (ed. by D. Eylon, R.R. Boyer and D.A. Koss), 227.
[21] G. Ghosh and G.B. Olson: *Acta. metall. mater.,* 1994, **42**, 3361-3370.
[22] P.E.J. Rivera-Díaz-del-Castillo, P. Di Napoli, Suresh Neelakantan and S. van der Zwaag: 'Ti-2007 Science and Technology (JIMIC5)', The Japan Institute of Metals, Kyoto, 2007, (ed. by M. Ninomi, S. Akiyama, M. Ikeda, M. Hagiwara, K. Maruyama), 471.
[23] T.O. Sato, S. Hukai and Y.C. Huang: *J. Aust. Inst. of metals*, 1960, **5**, 149-153.
[24] P. Duwez: *Trans. ASM*, 1953, **45**, 934-940.
[25] K.S. Jepson, A.R.G. Brown and J.A. Gray: 'The Science, technology and application of Titanium', Pergamon Press, London, 1970, (ed. by R.I. Jaffee and N. Promisel), 677.
[26] E. J. Melero, N.H. van Dijk, L. Zhao, J. Sietsma, S.E. Offerman, J.P. Wright and S. van der Zwaag: *Scripta Mater.*, 2007, **56**, 421-424.
[27] J.J. Wang and S. van der Zwaag: *Metall. Mater. Trans.A*, 2001, **32A**, 1527-1539.
[28] Q. Furnémont, M. Kemp, P.J. Jacques, M. Göken and F. Delannay: *Mater. Sci. Eng. A*, 2002, **328**, 26-32.

List of Tables

Table 1. Chemical analysis of the alloy (wt.%)

Material	Elements						
	V	Al	Fe	O	N	C	Ti
Ti-10V-2Fe-3Al	9.8	3	1.9	0.11	0.01	0.007	balance

Table 2. Heat treatments performed on Ti-10V-2Fe-3Al alloy:

Temperature domain	Heat treatment schemes		Cooling Mode	Microstructural features
	Temperature (°C)	Soaking time (min)		
β	900	1.5, 15, 60, 120 and Overnight	He gas quench	β, athermal martensite
	1000	1.5 and 15	He gas quench	β, athermal martensite
	1100	1.5, 15 and 60	He gas quench	β, athermal martensite at grain boundaries
	800	15	He gas quench	β, athermal martensite & α flakes
$\alpha+\beta$	700	15	He gas quench	β, α (flakes & spheroids)
$\beta + (\alpha + \beta)$	900	60	Cool	β, α (Widmanstätten, flake morphologies) & athermal martensite
	+ 750	60	He gas quench	
	900	60	Cool	β, α (Widmanstätten, flake morphologies)
	+ 650	60	He gas quench	
	900	60	Cool	β, α (Widmanstätten, flake morphologies) & athermal martensite
	+ 700	15 and 60	He gas quench	
	900	15	Cool	β, α (Widmanstätten, flake morphologies)
	+ 650	15 and 60	He gas quench	
	900	15	Cool	β, α (Widmanstätten, flake morphologies) & athermal martensite
	+ 750	15 and 60	He gas quench	
	900	15	Cool	β, α (Widmanstätten, flake morphologies) & athermal martensite
	+ 700	15 and 60	He gas quench	

* Heating and cooling rate is 10 °C/s

Table 3. Lattice parameters of the different phases:

		Lattice parameters (Å) Heat treated			Lattice parameters (Å) Compressed		
		Sample A	Sample B	Sample C	Sample A	Sample B	Sample C
β (BCC)	*a*	3.2433	3.2339	3.2355	3.2378	3.2439	3.231
α (HCP)	*a*		2.933	2.9396		2.933	2.929
	c		4.6764	4.6582		4.6723	4.457
α′ (HCP)	*a*	2.9190		2.9532	2.885		2.8813
	c	4.6770		4.4887	4.638		4.643
α″ (Orthorhombic)	*a*	3.02		2.9992	3.02		2.97
	b	4.985		4.9222	4.95		4.983
	c	4.356		4.3598	4.4221		4.3984

List of Figures

Figures

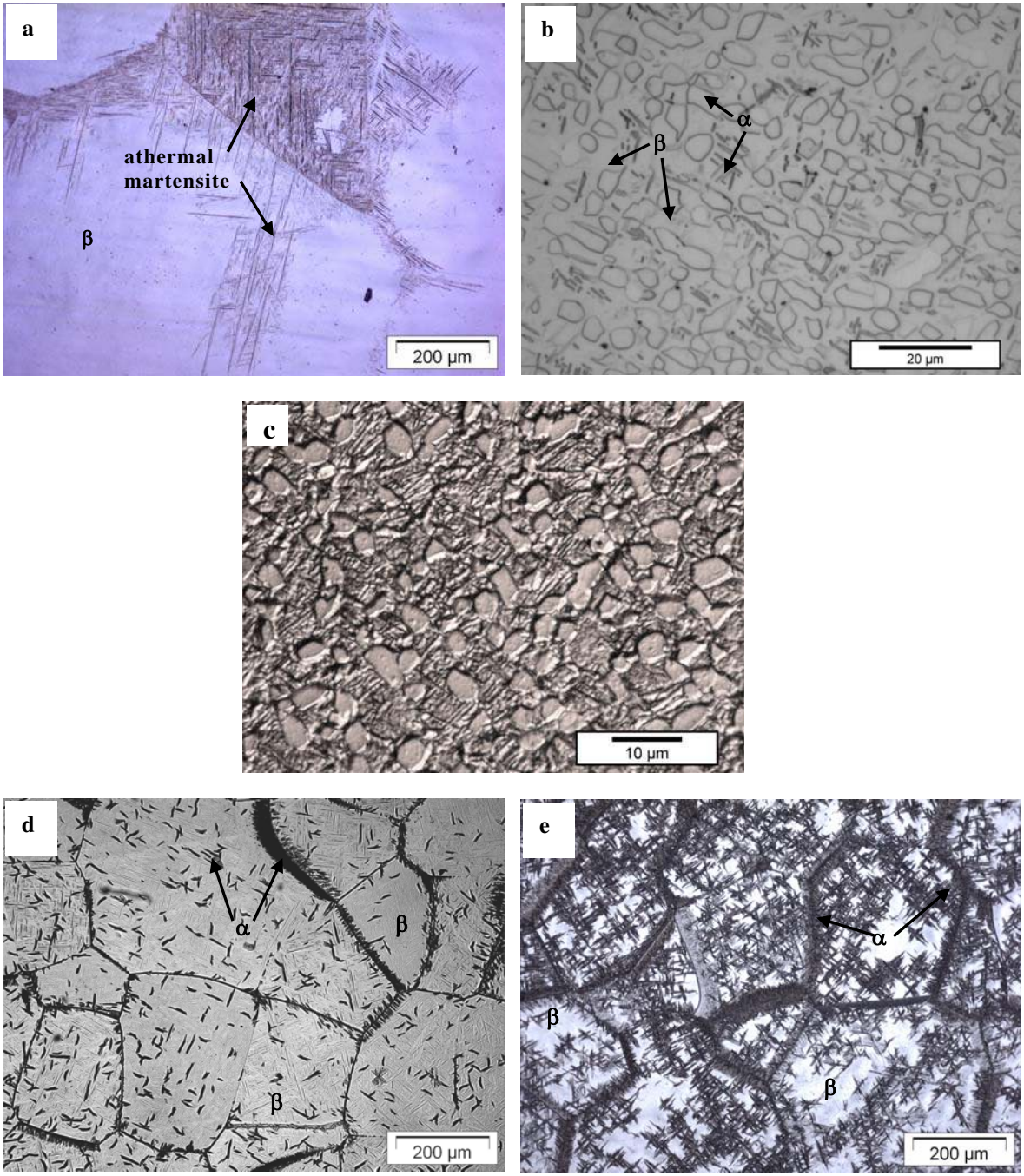

Figure 1. Micrographs of the different heat treated samples showing a) β with athermal martensite (900 °C-60min); b) α and β bi-modal structure (700 °C-15min); c) α and β bi-modal structure (as-received); d) β, athermal martensite, lower amount of intragranular α laths, and intergranular Widmanstätten structure (900 °C-15min/700 °C-15min) and e) β, intragranular α laths and intergranular Widmanstätten structure (900 °C-15min/650 °C-15min)

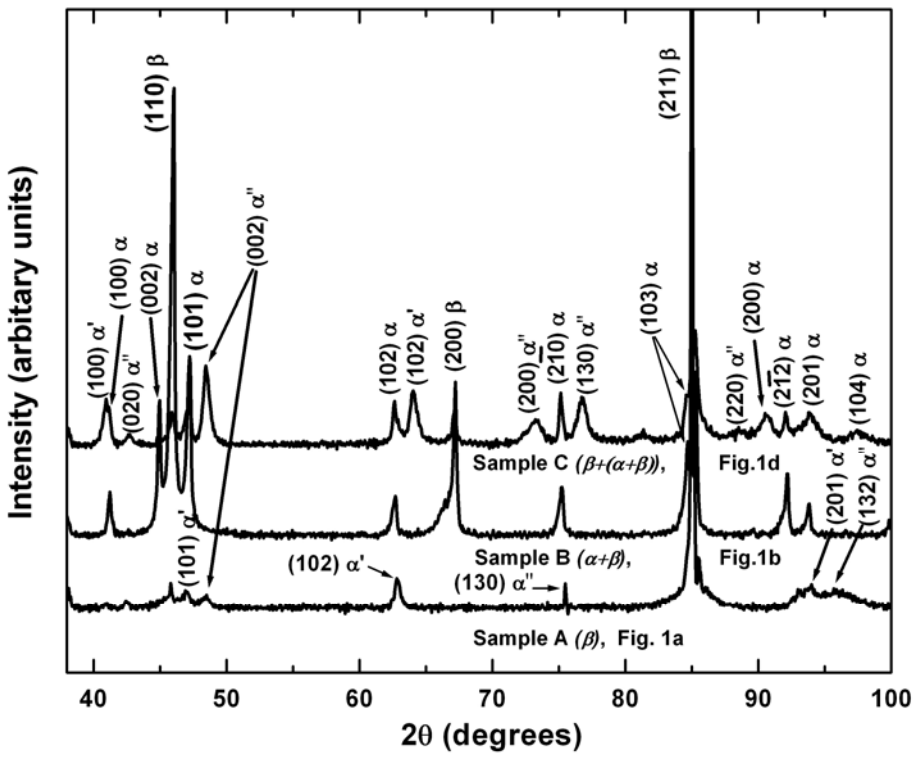

Figure 2. Diffractograms of the Ti-1023 alloy for different heat treated conditions

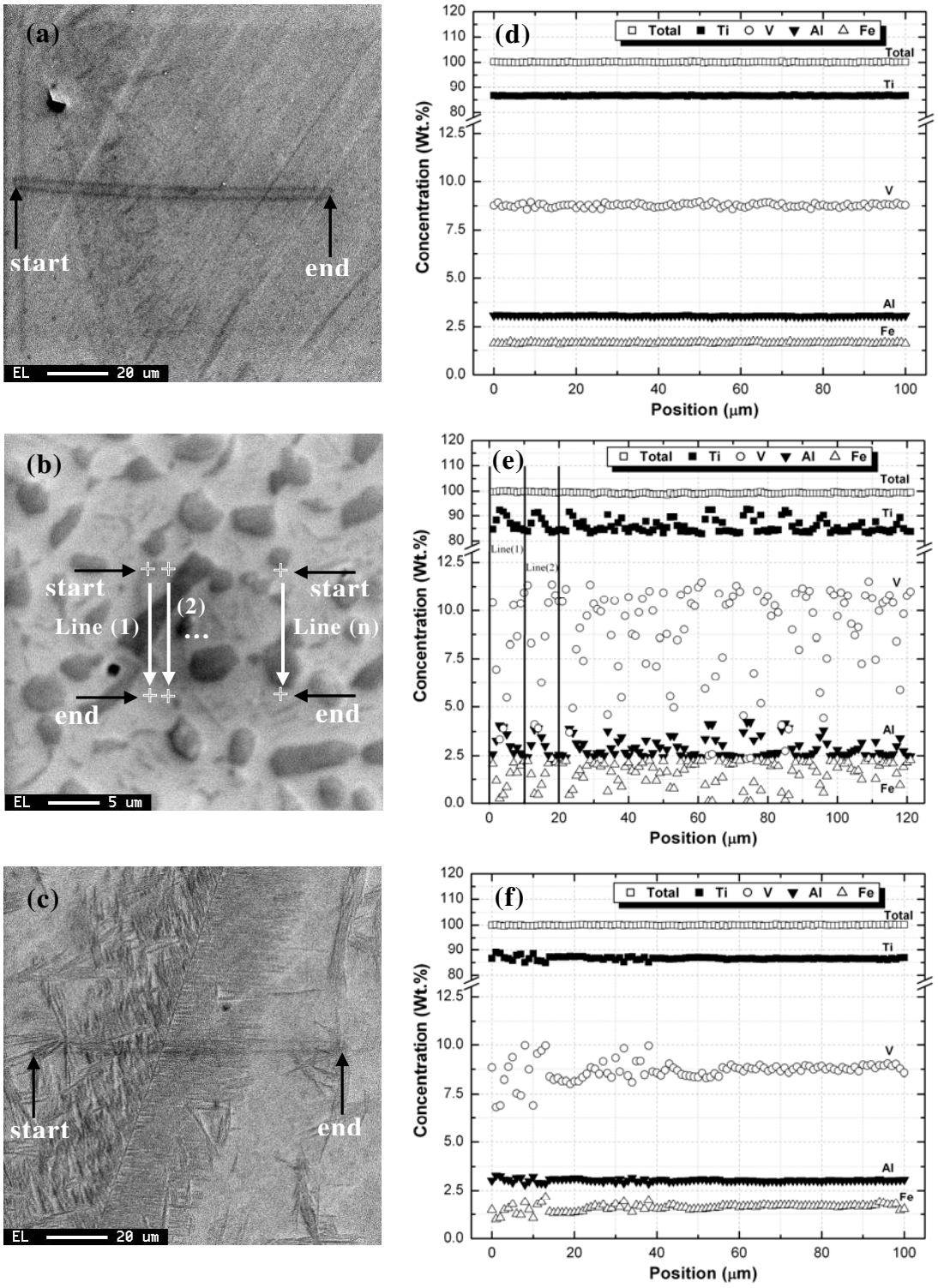

Figure 3. EPMA measurements in a region of the heat treated microstructures of (a) Sample A (900 °C-60min) (b) Sample B (700 °C-15min), probe measurements were carried out as series of vertical parallel lines(line 1 till line n) (c) Sample D (900 °C-15min/650 °C-15min); and (d),(e),(f) show the resultant concentration variations, respectively.

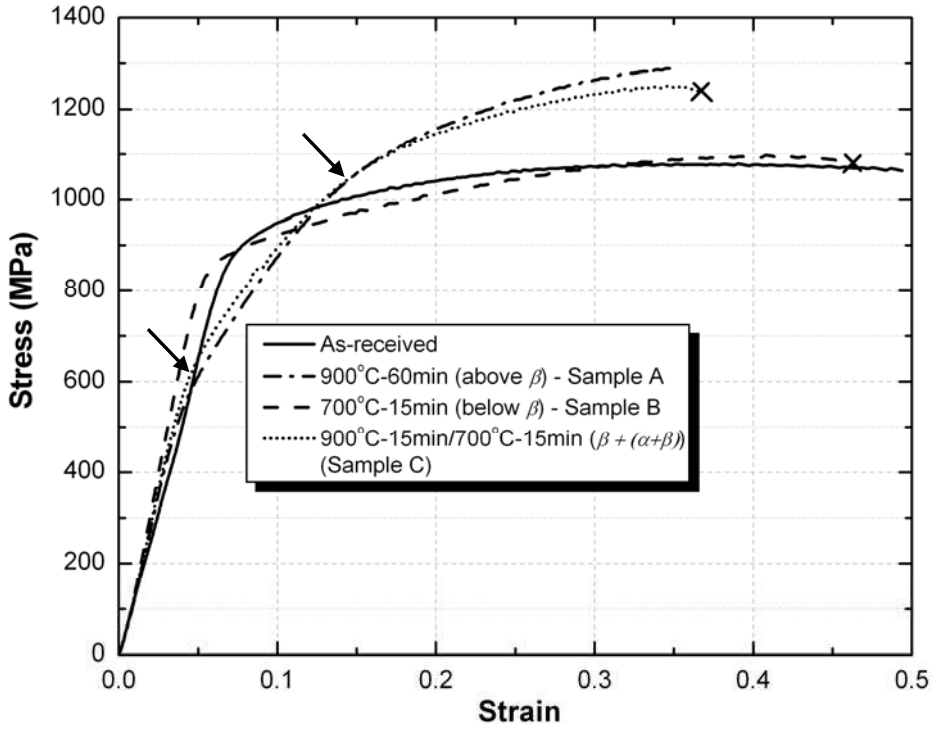

Figure 4. Compressive Stress-Strain curves of samples A, B and C; arrow indicates the double yield point behaviour associated to SIM formation

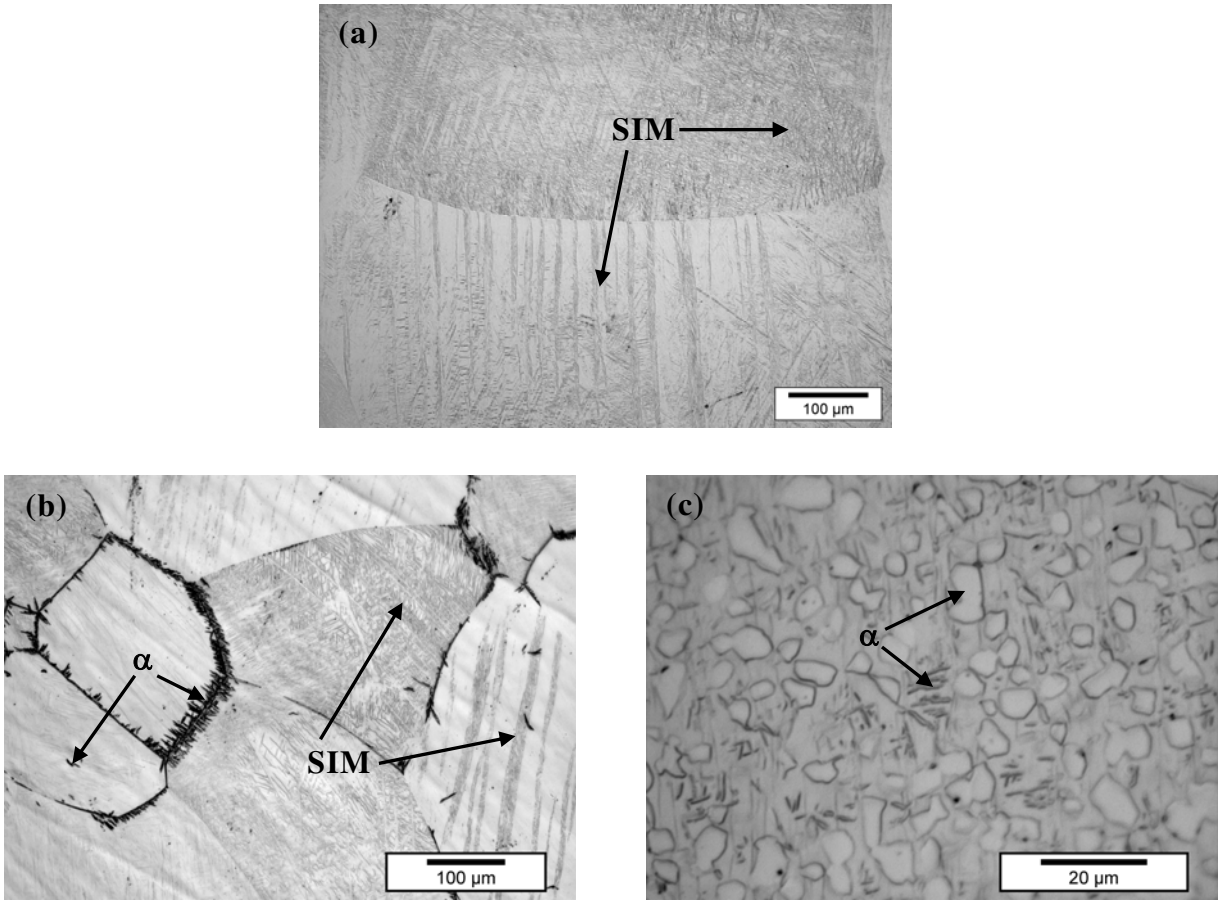

Figure 5. Micrographs of (a) ~35% compressed Sample A (above β) (b) ~20% compressed Sample C $(\beta+(\alpha+\beta)$ (c) ~20% compressed Sample B (below β)

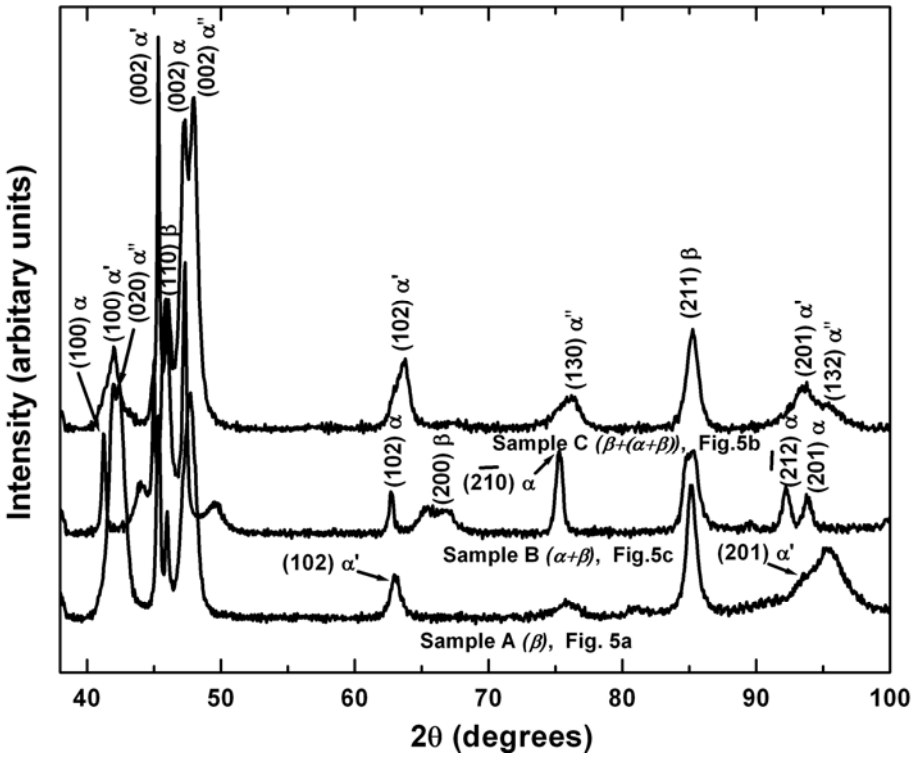

Figure 6. X-ray diffraction of compression tested Samples A, B and C.

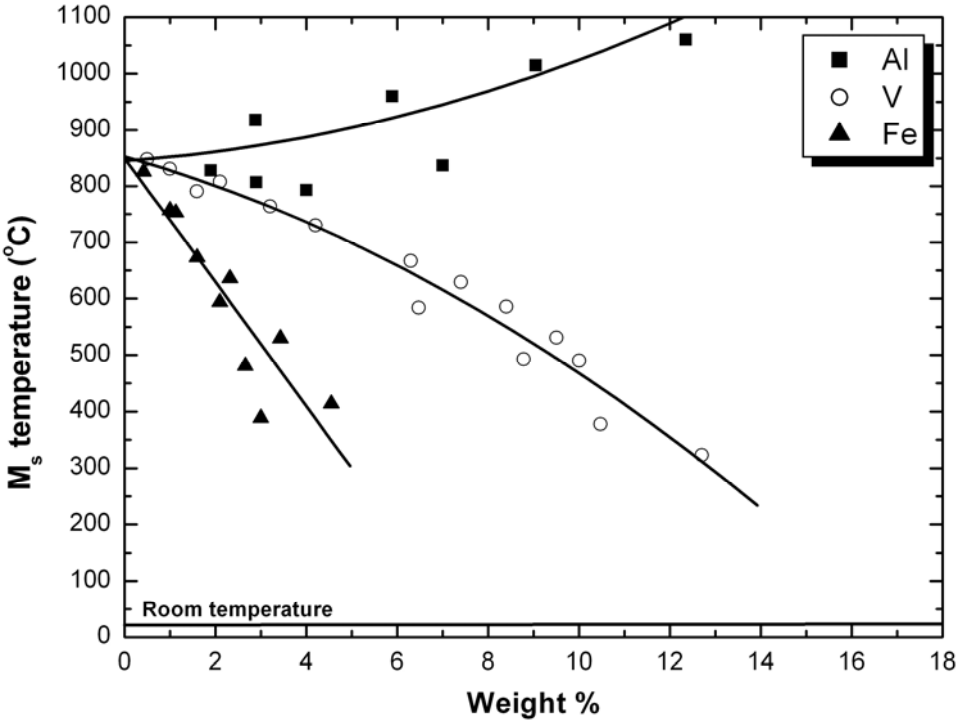

Figure 7. Concentration dependence of M_s temperature for the binary elements (Ti-V, Ti-Fe and Ti-Al) of Ti-1023 alloy.[23-25]